Cell PRESS
Chemistry & Biology
Article

The Role of Glutathione S-Transferase GliG in Gliotoxin Biosynthesis in *Aspergillus fumigatus*

Carol Davis,[1] Stephen Carberry,[1] Markus Schrettl,[1] Ishwar Singh,[2] John C. Stephens,[2] Sarah M. Barry,[3] Kevin Kavanagh,[1] Gregory L. Challis,[3] Dermot Brougham,[4] and Sean Doyle[1,*]
[1]Department of Biology and National Institute for Cellular Biotechnology
[2]Department of Chemistry
National University of Ireland Maynooth, Maynooth, Co. Kildare, Ireland
[3]Department of Chemistry, University of Warwick, Coventry CV4 7AL, UK
[4]School of Chemical Sciences, Dublin City University, Glasnevin, Dublin 9, Ireland
*Correspondence: sean.doyle@nuim.ie
DOI 10.1016/j.chembiol.2010.12.022

SUMMARY

Gliotoxin, a redox-active metabolite, is produced by the opportunistic fungal pathogen *Aspergillus fumigatus*, and its biosynthesis is directed by the *gli* gene cluster. Knowledge of the biosynthetic pathway to gliotoxin, which contains a disulfide bridge of unknown origin, is limited, although L-Phe and L-Ser are known biosynthetic precursors. Deletion of *gliG* from the *gli* cluster, herein functionally confirmed as a glutathione S-transferase, results in abrogation of gliotoxin biosynthesis and accumulation of 6-benzyl-6-hydroxy-1-methoxy-3-methylene-piperazine-2,5-dione. This putative shunt metabolite from the gliotoxin biosynthetic pathway contains an intriguing hydroxyl group at C-6, consistent with a gliotoxin biosynthetic pathway involving thiolation via addition of the glutathione thiol group to a reactive acyl imine intermediate. Complementation of *gliG* restored gliotoxin production and, unlike *gliT*, *gliG* was found not to be involved in fungal self-protection against gliotoxin.

INTRODUCTION

The biosynthesis of fungal secondary metabolites frequently involves nonribosomal peptide synthetases and a range of associated enzymes that is often encoded by gene clusters (Maiya et al., 2006; Stack et al., 2007). An example of one such nonribosomal peptide made by fungi is the epipolythiodioxopiperazine (ETP), gliotoxin **1** (Figure 1), which contains a transannular disulfide bridge of unknown origin (Fox and Howlett, 2008). Primarily due to the disulfide bridge, gliotoxin exhibits antimicrobial, immunosuppressive, and antiangiogenic properties, and its various biological activities have been the subject of significant investigation (Bernardo et al., 2003; Li et al., 2006; Choi et al., 2007). It has also attracted attention as a biomarker of fungal disease and contaminated animal feedstuffs (Lewis et al., 2005; Pena et al., 2010).

The *gli* biosynthetic cluster, which directs gliotoxin production in *Aspergillus fumigatus*, was identified in 2004 and is now known to contain 13 genes (Gardiner et al., 2004; Schrettl et al., 2010). Subsequent work showed that the coordinated expression of constituent genes was associated with gliotoxin production, and targeted disruption of the genes encoding a transcriptional regulator (*gliZ*) and a nonribosomal peptide synthetase (*gliP*) abolished gliotoxin biosynthesis in *A. fumigatus* (Gardiner and Howlett, 2005; Cramer et al., 2006; Bok et al., 2006; Kupfahl et al., 2006). Biochemical studies of purified recombinant GliP demonstrate that it is capable of assembling an L-Phe-L-Ser dipeptidyl thioester intermediate tethered to a thiolation domain within the enzyme. This intermediate undergoes slow conversion to the corresponding diketopiperazine **2**, which is probably the first free intermediate in gliotoxin biosynthesis (Balibar and Walsh, 2006) (Figure 1). Although the gene encoding the proposed ABC transporter export system for gliotoxin (*gliA*) has not been disrupted in *A. fumigatus*, deletion of an ortholog, *sirA*, in *Leptosphaeria maculans* surprisingly resulted in increased secretion of sirodesmin, an ETP structurally related to gliotoxin (Gardiner et al., 2005a). The *sirA* mutant exhibited increased sensitivity to exogenous sirodesmin and gliotoxin, and expression of *gliA* from *A. fumigatus* in *L. maculans* Δ*sirA* conferred resistance to gliotoxin, but not sirodesmin. More recently, a flavin-dependent oxidoreductase, encoded by *gliT* within the gliotoxin biosynthetic gene cluster, has been shown to completely protect *A. fumigatus* against exogenous gliotoxin (Schrettl et al., 2010; Scharf et al., 2010). Gliotoxin production was also abrogated in a *gliT* mutant of *A. fumigatus* and transformation of *A. nidulans* and *Saccharomyces cerevisiae*, respectively, with *gliT* conferred gliotoxin resistance on these gliotoxin-sensitive fungal species (Schrettl et al., 2010). Biochemical studies with purified recombinant GliT show that it catalyzes transannular disulfide formation in the dithiol precursor **3**, which is the final step in gliotoxin biosynthesis (Scharf et al., 2010).

The role of other genes within the gliotoxin biosynthetic gene cluster, either in self-protection against, or biosynthesis of, gliotoxin, remains to be fully elucidated (Gardiner et al., 2005b). In particular the origin and mechanism of incorporation of the sulfur atoms into gliotoxin are unclear. Although it has been demonstrated that [3,3-$^2H_2$]L-tyrosine, [3,3-$^2H_2$]O-prenyl-L-tyrosine, [3,3,5′,5′,5′-$^2H_5$]O-prenyl-L-tyrosine, and [5,5-$^2H_2$]phomamide can be incorporated into sirodesmin PL, it has not been possible to conclusively identify—by feeding studies with isotope-labeled precursors—the metabolic origin of the sulfur atoms in this ETP (Pedras and Yang, 2009). The diketopiperazine alkaloid

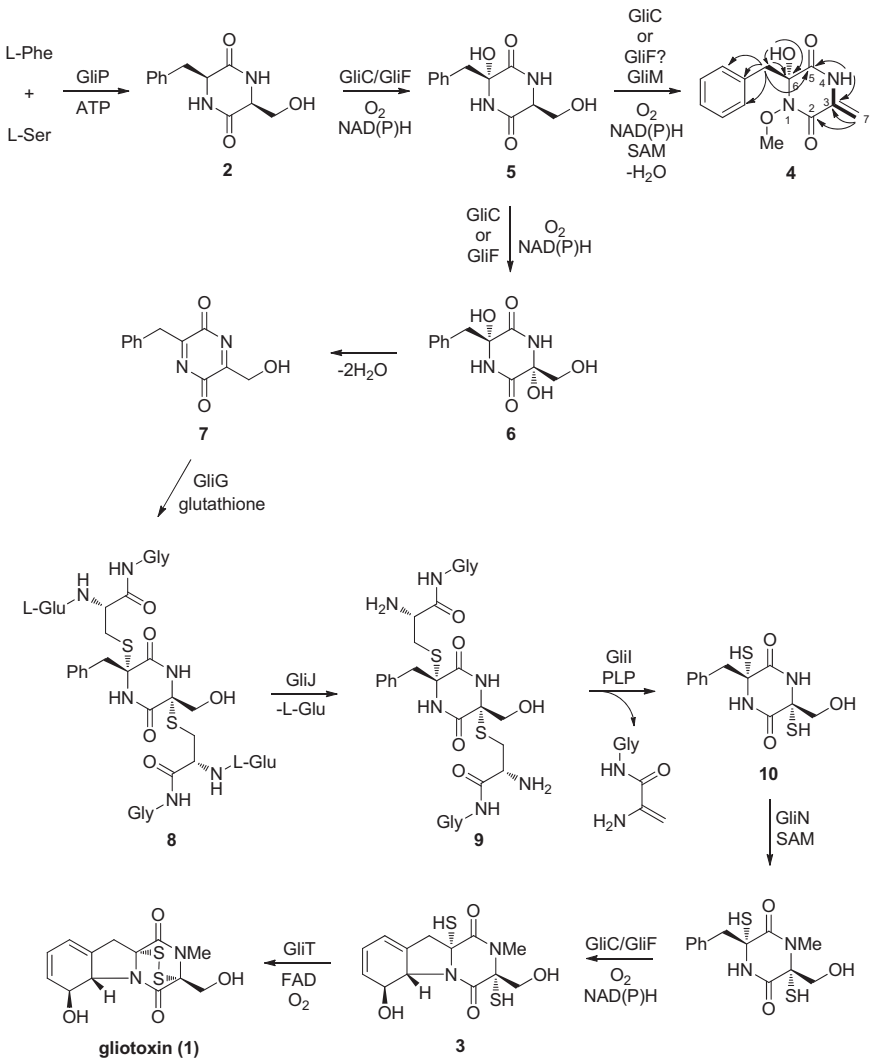

Figure 1. Proposed Biosynthetic Pathway for Gliotoxin Biosynthesis

Following GliP-mediated conjugation of L-Phe and L-Ser (Balibar and Walsh, 2006), a series of hydroxylation and dehydration reactions result in reactive acyl imine intermediate formation. Thiolation (GliG-mediated using GSH), possibly followed by sequential GliJ peptidase and GliI thioesterase activity, then occurs to yield the sulfurized intermediate. Subsequent tailoring reactions lead to gliotoxin **1** formation. Compound **4** is isolated as an off-pathway metabolite as a result of intermediate instability following *gliG* deletion. See also Figures S2–S9.

(+)-11,11′-dideoxyverticillin A, which contains two transannular disulfide bridges, is produced by *Penicillium* sp. The total chemical synthesis of this ETP has recently been achieved (Kim et al., 2009), in which late-stage treatment of a protected bis-dihydroxydiketopiperazine intermediate with K_2CS_3 results in the formation of a dimeric bisdithiepanethione, in high yield, presumably via initial elimination of water to form an acyl iminium ion intermediate followed by addition of CS_3^{2-}, resulting ultimately in the replacement of four C-O bonds with four C-S bonds. This study demonstrates that biosynthetic incorporation of sulfur into ETPs via diketopiperazine C-hydroxylation and subsequent elimination of water to form an acyl imine that undergoes addition of a thiol is chemically feasible.

The role of *gliG* (AFUA_6G09690; http://www.cadre-genomes.org.uk/) within the *gli* cluster, which in silico analysis predicts encodes a glutathione S-transferase (GST), is unclear. It could be involved in biosynthetic thiolation of an acyl imine intermediate or auto-protection against gliotoxin (Figure 1). Normally, GSTs catalyze conjugation of glutathione (GSH) to toxic (chemically reactive) metabolites to facilitate detoxification and cellular secretion. Although GSTs have received significant attention in mammalian and plant systems (Hayes et al., 2005; Dixon et al., 2010), their presence and function in fungi have only recently been studied (Burns et al., 2005; Morel et al., 2009). The low-percentage sequence identity of GliG to other putative GSTs encoded within the *A. fumigatus* genome (Cramer et al., 2006) (approximately 30%) may indicate a function for GliG that is distinct from the other GSTs (Nierman et al., 2005). To investigate the function of *gliG* in *A. fumigatus*, it was disrupted, and the phenotype of the mutant with respect to gliotoxin biosynthesis and auto-protection was examined.

RESULTS

Deletion and Complementation of *gliG* in *A. fumigatus*

Homologous transformation using the bipartite marker technique (Nielsen et al., 2006), with modifications, was used to generate Δ*gliG* mutants in both *A. fumigatus* Δ*akuB* (da Silva Ferreira et al., 2006) and AF293 (Nierman et al., 2005) backgrounds. Here, the *A. fumigatus* strains were cotransformed with two DNA constructs, each containing an incomplete fragment of the pyrithiamine (*ptrA*) resistance gene (Kubodera et al., 2000) fused to 1.2 kb (5′) and 1.0 kb (3′) of *gliG*-flanking sequences (Figure 2). These constructs were generated by PCR and characterized by DNA sequence analysis that confirmed the replacement of *gliG* by overlapping *ptrA* regions on intact 5′ and 3′-flanking regions, respectively. Southern analysis was used to screen 37 putative transformants for *gliG* (negative) and *ptrA* (positive) colonies with a 2124 bp XbaI restriction fragment in place of the wild-type 1668 bp XbaI restriction fragment (Figure 2). This led to identification of a *gliG* mutants (*A. fumigatus* $\Delta gliG^{akuB}$ and $\Delta gliG^{AF293}$). Complementation of the *A. fumigatus* $\Delta gliG^{AF293}$ mutant was achieved by transformation with a vector containing intact *gliG* and the phleomycin resistance gene using selection on phleomycin-containing media. Southern analysis of the complemented strains produced the expected EcoRV restriction fragments of 3.4 and 1.5 kb, respectively (Figure 2).

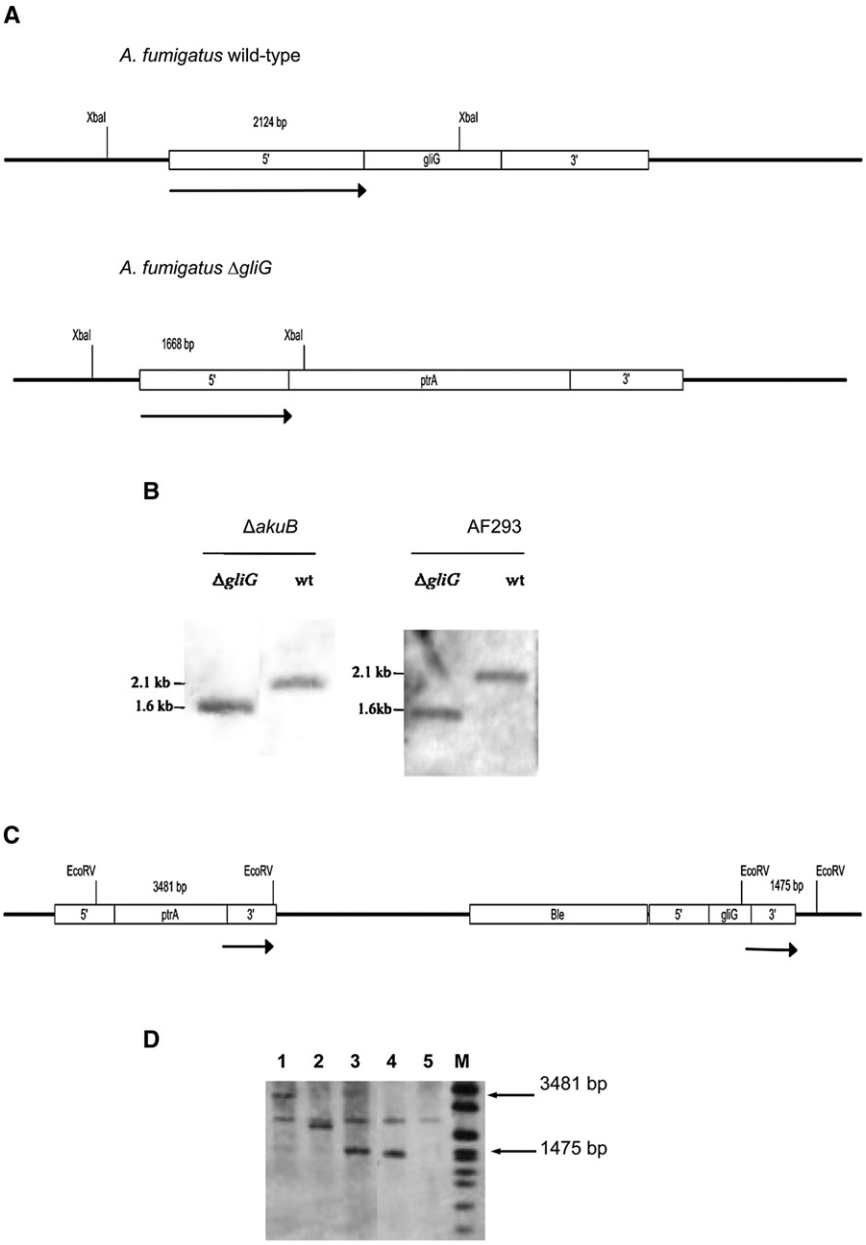

Figure 2. Deletion and Complementation of *gliG* in *A. fumigatus* Δ*akuB* and AF293, Respectively

(A) Representation of the *gliG* locus in wild-type and Δ*gliG* mutant strains. In Δ*gliG* mutant strains an 828 bp internal section of the *gliG* coding region was replaced with 2.0 kb *ptrA* from pSK275 vector. An XbaI restriction enzyme was used to digest genomic DNA, which was probed with a 1.2 kb probe.

(B) Southern analysis of Δ*gliG* mutant versus wild-type DNA for *A. fumigatus* Δ*akuB* and AF293, respectively. Here, a DIG-labeled probe amplified using ogliG-3 and ogliG-6 for the 5′-flanking region was used to detect the predicted presence of 1.6 and 2.1 kb fragments in XbaI-digested genomic DNA from Δ*gliG* and wild-type, respectively.

(C) Representation of the Δ*gliG* locus in complemented strains (*gliG*^{C}). A linearized plasmid (p*gliG-phleomycin*) was transformed into the Δ*gliG* locus. Genomic DNA of the complemented strains was digested with EcoRV, and probed using a 1 kb probe.

(D) Southern analysis of Δ*gliG* complemented strains (*gliG*^{C}). A DIG-labeled probe amplified using ogliG-4 and ogliG-5 for the 3′-flanking region was used to detect the presence of a 3.4 and 1.5 kb fragment in EcoRV-digested genomic DNA. Lanes 1 and 3 represent transformant Nos. 15 and 17, respectively. Both contain the predicted 3.4 and 1.5 kb fragments. These transformants were isolated as potential complemented strains and subjected to second-round Southern analysis to confirm this complementation. Lane 2 represents a transformant that was not deemed as complemented. Lane 4 is wild-type DNA that contains the predicted fragment of 1.5 kb. Lane 5 is Δ*gliG* DNA that was expected to contain neither the 3.4 or the 1.5 kb signal.

These complemented strains (*gliG*^{C}), termed 15.1, 15.4, and 17.1, exhibited wild-type features in all subsequent experiments. Northern analysis confirmed that *gliG* transcripts are absent from Δ*gliG*^{akuB} and Δ*gliG*^{AF293} but present in *A. fumigatus* wild-type and *gliG*^{C} (Figure 3).

Phenotypic Analysis

Exposure of *A. fumigatus* wild-type and Δ*gliG* conidia to exogenous gliotoxin (10–50 μg/ml) showed that both strains grew equally well (Figure 4), thereby confirming that *gliG* does not play a role in self-resistance to gliotoxin. Observation of *A. fumigatus* wild-type and Δ*gliG* conidia in the presence of H_2O_2 (1, 2, and 5 mM), voriconazole (0.15 and 0.25 μg/ml), and amphotericin B (1, 2, and 5 μg/ml) showed that both wild-type and mutant grew at identical rates (data not shown), thus excluding *gliG* involvement in protection against oxidative stress and antifungal agents. Exposure to conidia of *A. fumigatus* Δ*gliG* induced greater melanization in the *Galleria mellonella* virulence model (Reeves et al., 2004) compared to wild-type or *gliG*^{C} (15.1, 15.4, and 17.1), although no statistical significance was observed in overall virulence among wild-type, mutant, or complemented strains (data not shown).

A. fumigatus Δ*gliG* Does Not Produce Gliotoxin

Organic extracts from 48-hr cultures of *A. fumigatus* wild-type, Δ*gliG*$^{\Delta akuB}$, Δ*gliG* ^{AF293}, and *gliG*^{C} were prepared and analyzed by LC-ToF MS (Figure 5) and comparative RP-HPLC analysis (see Figure S1 available online). It is clear from Figure 5 that although gliotoxin was produced (mean ± SD: 784.9 ± 869.88 μg/ml) by *A. fumigatus* wild-type (retention time [R_T] = 14.8 min, Figure S1), no gliotoxin was detectable in organic extracts from the *A. fumigatus* Δ*gliG* strains. However, an alternative metabolite, termed M12.3, was evident in Δ*gliG* organic

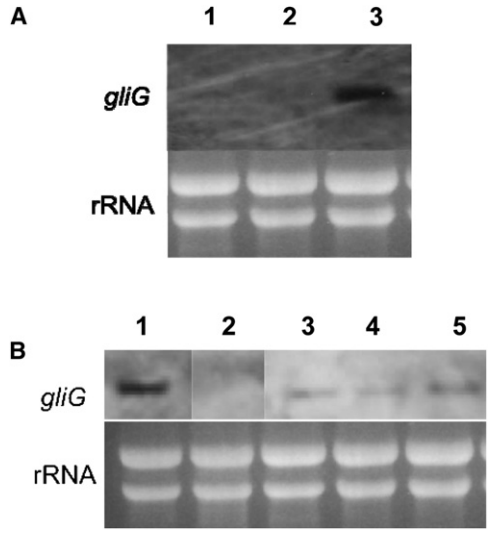

Figure 3. Expression Analysis of *gliG* in *A. fumigatus*

(A) Absence of *gliG* expression was confirmed in *A. fumigatus* $\Delta gliG^{\Delta akuB}$ by northern analysis. Wild-type (lane 1) and Δ*gliG* (lane 2) cultures were grown for 21 hr, followed by gliotoxin addition (3 hr). Wild-type (lane 3) ATCC46645 cultures were grown for 48 hr in AMM. Northern analysis was performed, and absence of *gliG* expression in $\Delta gliG^{\Delta akuB}$ is evident. Equal RNA loading/track was shown by rRNA subunit presence.

(B) Northern blot analysis of *gliG* expression in *A. fumigatus* AF293, $\Delta gliG^{AF293}$, and $gliG^{C}$. Lane 1 corresponds to *A. fumigatus* RNA extracts from 48-hr AMM for AF293 wild-type. Lane 2 shows RNA extracts from 48-hr AMM for *A. fumigatus* $\Delta gliG^{AF293}$. Lanes 3–5 correspond to *A. fumigatus* RNA extracts from 48-hr AMM for three independent *gliG*-complemented strains. Equal RNA loading/track was shown by rRNA subunit presence.

extracts, with R_T = 12.3 min (Figure 6). LC-ToF MS analysis also confirmed the restoration of gliotoxin production in $gliG^{C}$ (Figure 5) (range: 2244 ± 1622 μg/ml to 3158 ± 63.57 μg/ml).

Sequential $NaBH_4$ reduction (Woodcock et al., 2001) and alkylation (5′-iodoacetamidofluorescein; 5′-IAF) of organic extracts from *A. fumigatus* wild-type, Δ*gliG*, and $gliG^{C}$ was undertaken. Gliotoxin was completely reduced to the dithiol form using sodium borohydride. The presence of di-acetamido-fluorescein-gliotoxin (GT-$(AF)_2$) was evident in organic extracts from *A. fumigatus* wild-type (Figure 5) and $gliG^{C}$ (Figure S1). However, no 5′-IAF-labeled gliotoxin was detectable, with or without prior reduction, in organic extracts derived from *A. fumigatus* $\Delta gliG^{AF293}$ (Figure 5). This confirmed the absence of free thiols or a disulfide bridge in M12.3 and suggested that GliG may play a role in the incorporation of sulfur atoms into gliotoxin.

A Gliotoxin Biosynthetic Shunt Metabolite Is Secreted by *A. fumigatus* Δ*gliG*

LC-ToF MS analyses of organic extracts of *A. fumigatus* $\Delta gliG^{AF293}$ indicated the presence of a compound (M12.3) with m/z = 263.1 that was absent from wild-type *A. fumigatus* and the complemented *gliG* mutant (Figure 6). Subsequent high-resolution LC-ToF MS analysis of M12.3, purified by preparative TLC (Figures 6A–6C), gave the molecular formula $C_{13}H_{14}N_2O_4$ for this compound (m/z calculated for $C_{13}H_{15}N_2O_4^+$: 263.1026; m/z found: 263.1027) (Figure 6D). The compound is proposed to be 6-benzyl-6-hydroxy-1-methoxy-3-methylenepiperazine-2,5-dione **4** (Figure 1), on the basis of NMR spectroscopic analysis.

Analysis of ^1H and ^{13}C, DEPT, COSY, HMBC, and HMQC spectra revealed that the compound contains two amide carbonyl groups (δ_c 1157.3, *C*ONH; 161.1, *C*ONOCH$_3$), a benzyl group (δ_c 46.5, *C*H$_2$Ph), a hydroxyl group at position 6 (δ_c 83.5, NHCO*C*(OH)Bn; δ_H 4.93, NHCOC(O*H*)Bn), a methoxy group (δ_c 62.2, O*C*H$_3$; δ_H 3.64, OC*H*$_3$), and a 1,1-disubstituted alkene (δ_c 100.1, C=*C*H$_2$; 134.2, *C*=CH$_2$; δ_H 5.00, 5.33, C=C*H*$_2$) (Figures 1 and Table 1; Figure S2–S9,). The proton of the hydroxyl group, at position 6, could be observed in the ^1H-NMR spectrum measured in CD_3CN, (δ_H 4.93 [NHCOC(O*H*)Bn]). This signal disappeared upon shaking with D_2O (Figure S3). We observed a δ_C value of 83.5 for C-6 of the compound that compares very favorably with reported δ_C values of 82.9 and 87.2 for the almost identical C-6 carbons in similar compounds (Buysens et al., 1996; King et al., 2003). In the ^1H-NMR spectrum in CD_3CN, the CON*H* proton signal at δ_H ~7.23 overlaps with the signals due to the aromatic protons, but in $CDCl_3$ the CON*H* signal is shifted away from the aromatic signals to δ_H 7.50. This shift in the CON*H* signal allowed us to distinguish between structure **4** and an alternative structure with the methoxy group attached to N-4 rather than N-1. The COSY spectrum in $CDCl_3$ showed a clear coupling between the CON*H* signal at δ_H 7.50 and the methylene protons (C = C*H*$_2$) (Figure 1; Figure S6). This long-range coupling, over four bonds, indicated that the NH group was located at position 4, adjacent to the disubstituted alkene (location of the NH group at position 1 would require a five bond coupling to the methylene protons). In addition the HMBC correlation data obtained in $CDCl_3$ showed a coupling between the CON*H* proton signal at δ_H 7.50 and C-5/C-3, (Figure 1 and Table 1), which is consistent with structure **4**. The alternative structure with the methoxy group at position 4 would be expected to show couplings between the CON*H* signal and C-2 and C-6 in the HMBC spectrum, which was not observed (Figure S9). Finally, no deep-violet color was observed when a ferric chloride test for the presence of hydroxamic acids was performed (Shin et al., 1975), confirming the absence of a hydroxamic acid group in the compound.

Feeding experiments with [3-^{13}C]-L-Phe and subsequent LC-ToF MS analysis strongly indicated that L-Phe is incorporated into **4** (Figure 6E). A substantial enhancement of the CH$_2$Ph signal in the ^{13}C-NMR spectrum of the labeled material (Figures S4B and S5B) confirmed L-Phe as a precursor of compound **4**. No uptake of compound **4** was detectable by RP-HPLC analysis in either *A. fumigatus* AF293 mycelia or protoplasts (data not shown). This precluded M12.3 **4** incorporation experiments in *A. fumigatus* wild-type.

Recombinant GliG Exhibits GST and Reductase Activity

Protein expression plasmid pPXA*gliG* consisting of the vector pProEx-Htb containing the coding sequence for *gliG* was used to transform *Escherichia coli* DH5α, and expression was induced by the addition of 0.6 mM IPTG. rGliG was present in cell lysate pellet, indicating insolubility, and was purified using differential extraction, with a yield of approximately 12 mg/g of *E. coli*. SDS-PAGE analysis confirmed a molecular mass of 25 kDa for

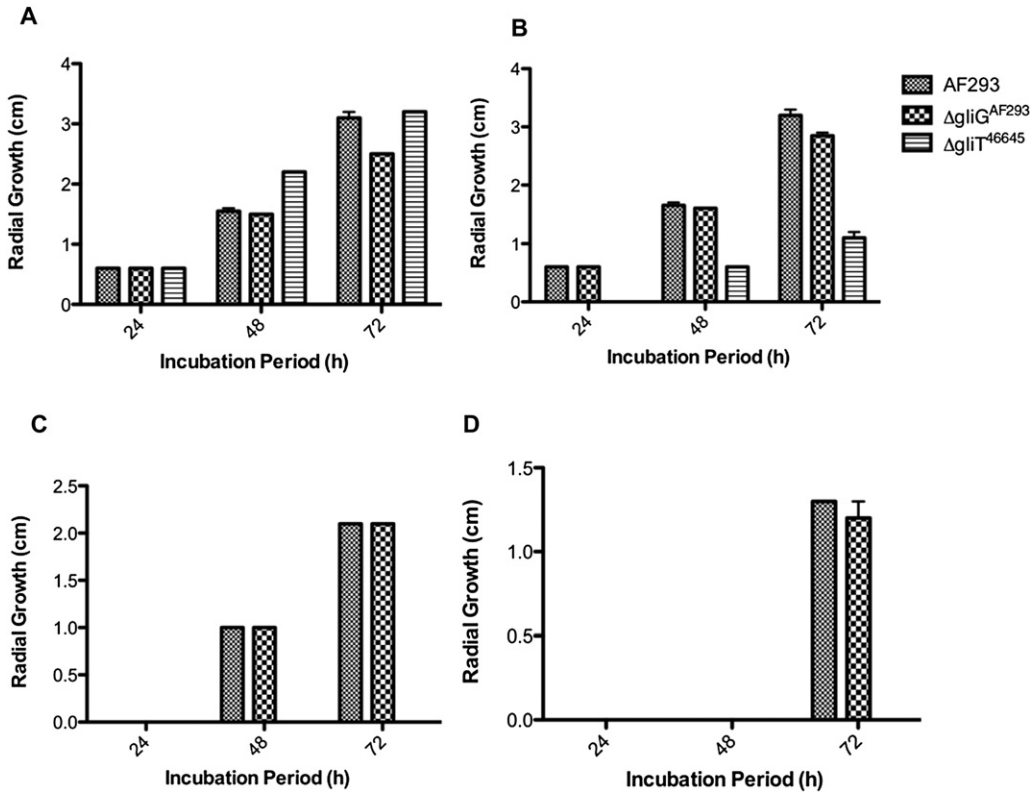

Figure 4. Effect of Gliotoxin on the Growth of *A. fumigatus* AF293, Δ*gliG*, and Δ*gliT*, Respectively

Radial growth (mean ± standard deviation) was measured up to 72 hr (n = 3). No statistically significant difference was observed on the effect of gliotoxin (0, 10, 30, and 50 μg/ml) (A–D) on *A. fumigatus* Δ*gliG* growth relative to wild-type.

rGliG (Figure S10). The identity of purified rGliG was confirmed by peptide mass fingerprinting. Several peptides corresponding to the theoretical protein sequence (26.5% sequence coverage; data not shown) were identified. Following large-scale overproduction, rGliG was solubilized and subjected to serial dialysis at 250 μg/ml, yielding 67% rGliG recovery (170 μg/ml). Post-dialysis, rGliG exhibited GST activity with 1,2-epoxy-3-(4-nitrophenoxy)-propane (EPNP Specific Activity [S.A.] [mean ± SD] = 2.3 ± 0.122 U/mg), 1-chloro-2,4-dinitrobenzene (CDNB S.A. = 0.20 ± 0.1 U/mg), and 3,4-dichloro-nitrobenzene (DCNB S.A. = 0.09 ± 0.001 U/mg). rGliG also exhibited glutathione reductase activity (S.A. = 0.01 ± 0.002 U/mg). Whole-protein lysates from *A. fumigatus* Δ*gliG*^{AF293} exhibited 17% less activity toward EPNP than those from *A. fumigatus* wild-type (S.A. = 0.12 ± 0.02 U/mg versus 0.145 ± 0.011 U/mg, respectively).

DISCUSSION

The biosynthetic pathway to gliotoxin has, before now, been unclear. Using a gene deletion strategy, our work has demonstrated that GliG, which exhibits GST activity and is encoded by a gene within the *gli* cluster, is essential for gliotoxin production in *A. fumigatus*. Furthermore, the absence of GliG results in the accumulation and secretion of the shunt metabolite 6-benzyl-6-hydroxy-1-methoxy-3-methylenepiperazine-2,5-dione **4**, which lacks both of the sulfur atoms incorporated into the disulfide bridge of gliotoxin. Genetic complementation of the *A. fumigatus gliG* mutant restored gliotoxin production. Unlike some of the other genes in the *gli* cluster studied to date (e.g., *gliT* or *gliA*), *gliG* is not involved in the auto-protection of *A. fumigatus* against exogenous gliotoxin. Taken together, our data suggest that GliG is involved in the introduction of sulfur into 6-benzyl-6-hydroxy-3-hydroxymethylpiperazine-2,5-dione **5** (Figure 1), the likely precursor of the shunt metabolite **4**.

The *gliG* gene was deleted from both *A. fumigatus* AF293 and *A. fumigatus* Δ*akuB* in order to elucidate its function in gliotoxin metabolism, a strategy noted by others for the functional dissection of the gliotoxin biosynthetic pathway (Patron et al., 2007; Fox and Howlett, 2008). Expression of *gliG*, along with other genes in the *gli* cluster, has been shown to be coincident with gliotoxin formation (Gardiner and Howlett, 2005). Moreover, Cramer et al. (2006) demonstrated that low-level *gliG* expression was evident in the *A. fumigatus* Δ*gliP* (termed ARC2) that, along with other *gli* cluster components (except *gliP*), was upregulated upon exposure to gliotoxin (20 μg/ml) for 24 hr. This has led to the suggestion that gliotoxin plays a role in the regulation of its own biosynthesis. Cramer et al. (2006) also observed entire *gli* cluster expression in *A. fumigatus* wild-type (AF293) in the presence of gliotoxin (20 μg/ml). In the present work, northern analysis confirmed the presence and absence of *gliG* expression in *A. fumigatus* AF293 and Δ*gliG*^{AF293}, respectively, in the absence

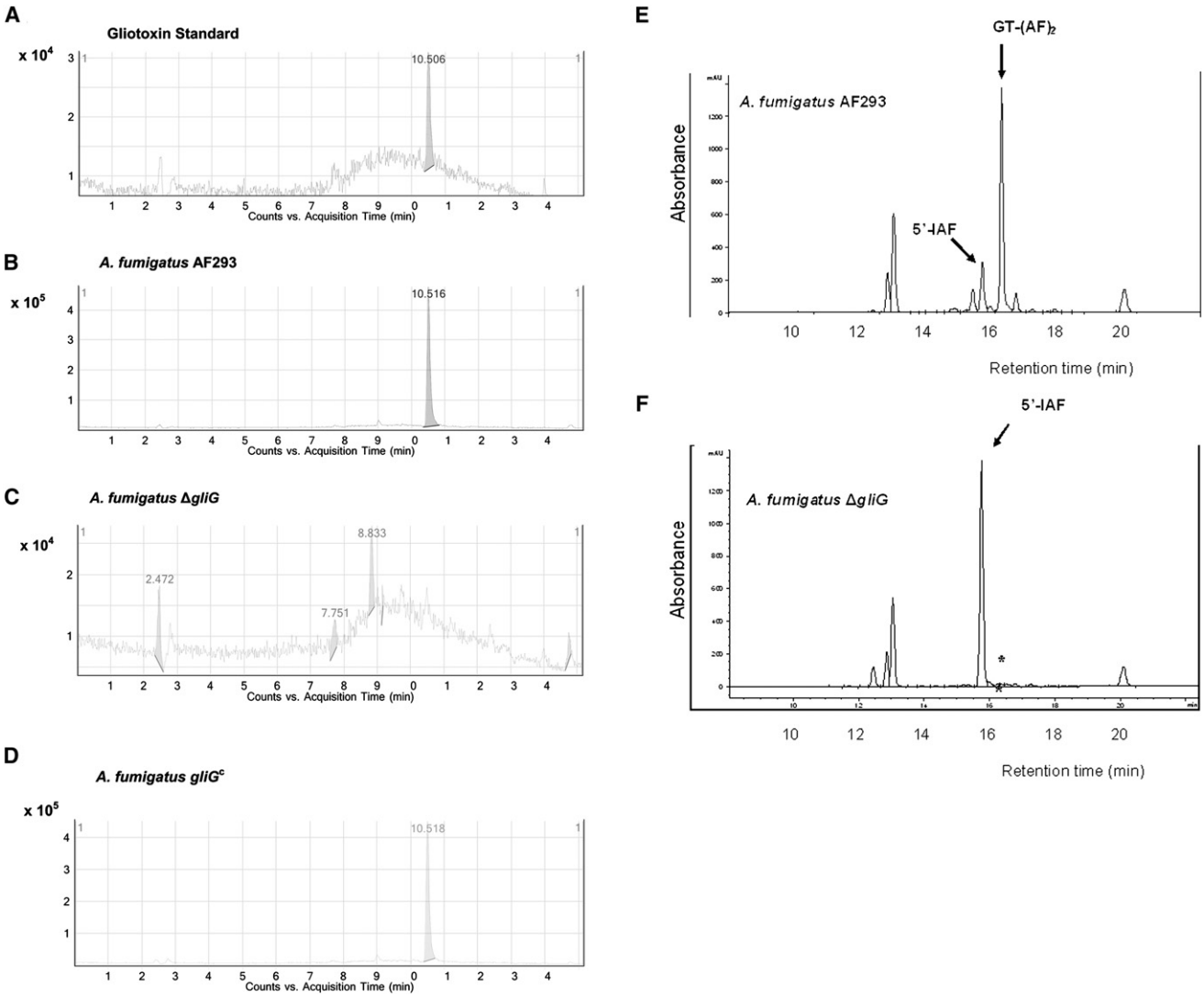

Figure 5. LC-ToF MS and RP-HPLC Analysis of *A. fumigatus* Strains Used in this Study

Chloroform extracts of culture supernatants of AMM cultures grown for 48 hr at 37°C. Gliotoxin and a putative biosynthetic intermediate were identified.

(A) Extracted ion chromatogram (EIC) following LC-ToF MS detection of gliotoxin standard (m/z = 327).

(B) *A. fumigatus* AF293 wild-type strain produced gliotoxin (EIC).

(C) *A. fumigatus* Δ*gliG* did not produce gliotoxin (EIC).

(D) *A. fumigatus* AF293 *gliG*^{C} 15.1 strain produced gliotoxin (EIC). Identical LC-MS results (not shown) were obtained from transformants *A. fumigatus* AF293 *gliG*^{C} 15.4 and 17.1, respectively.

(E) RP-HPLC analysis of reduced and alkylated gliotoxin present in organic extracts of culture supernatants from *A. fumigatus* AF293. The presence of di-acetamidofluorescein-gliotoxin (GT-(AF)$_2$) was evident.

(F) RP-HPLC analysis of reduced and alkylated gliotoxin present in organic extracts of culture supernatants from *A. fumigatus* Δ*gliG*^{AF293}. Absence of labeled gliotoxin was evident, as indicted by the asterisk.

See also Figure S1.

of added gliotoxin. However, gliotoxin addition was necessary to detect *gliG* expression in *A. fumigatus* Δ*akuB* wild-type, although no transcript was detectable in *A. fumigatus* Δ*gliG*^{akuB} by northern analysis. Coincident with absence of *gliG* expression, both *A. fumigatus* Δ*gliG* strains generated in this work were unable to produce gliotoxin, although a gliotoxin-related shunt metabolite (M12.3) **4** was identified in both deletion strains. Disruption of *gliP* and *gliZ*, respectively, also abrogates gliotoxin production. However, no gliotoxin-related metabolites were detected in these studies (Cramer et al., 2006; Kupfahl et al., 2006). Thus, our results extend the number of genes in the *gli* cluster confirmed to play a role in gliotoxin biosynthesis. Along with *gliG* expression, gliotoxin production was restored in *A. fumigatus* Δ*gliG*^{AF293} upon introduction of the entire *gliG* coding sequence. Interestingly, no *gliG*-complemented strains were recoverable from *A. fumigatus* Δ*gliG* disrupted in the *akuB* background. Bok et al. (2006) also observed restoration of gliotoxin production upon complementation of an

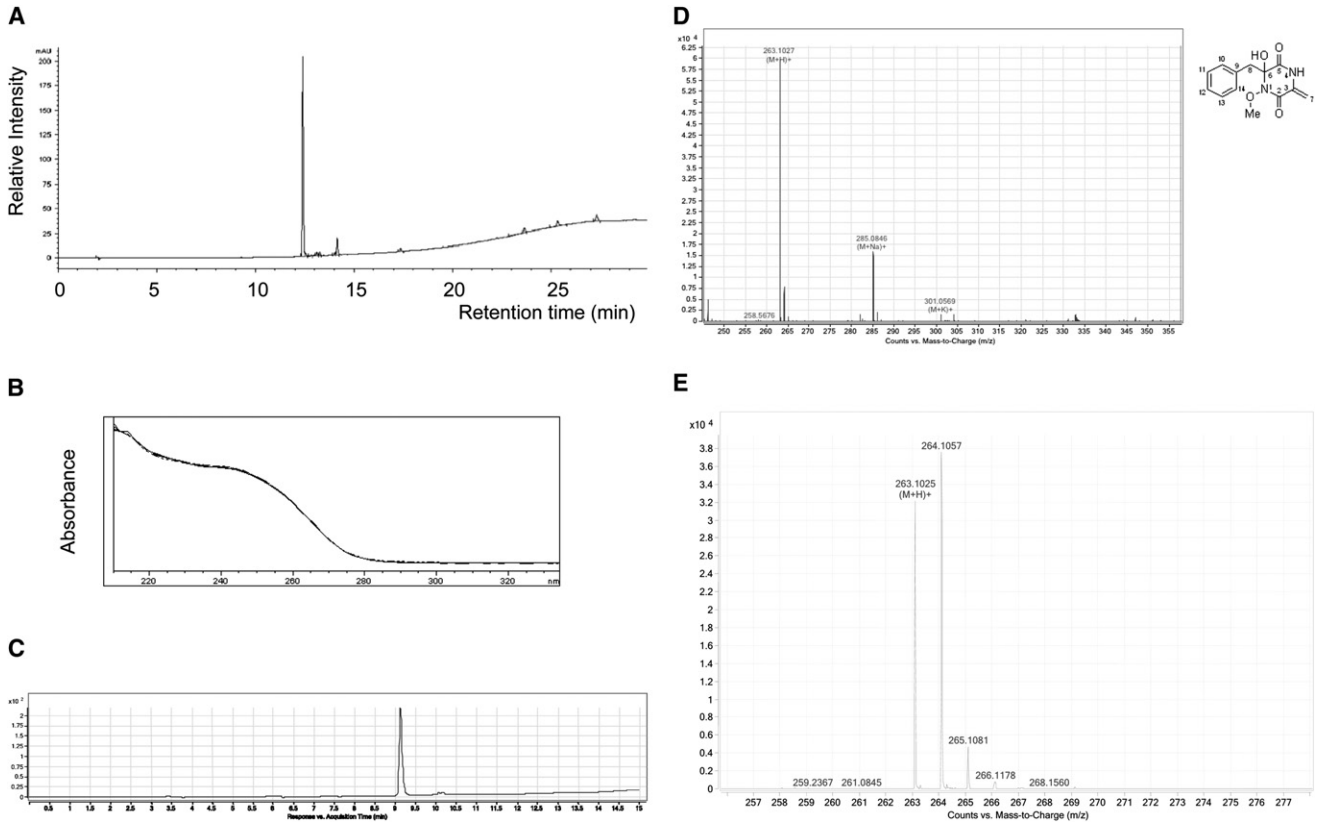

Figure 6. RP-HPLC (at A_{254nm}) and Spectrophotometric Analysis of the Purified Gliotoxin Biosynthetic Intermediate (M12.3) from *A. fumigatus* Δ*gliG*^{AF293}

(A) Chromatogram of purified M12.3 following organic extraction and TLC purification (injection volume: 20 μl; R_T = 12.383 min).

(B) Zoomed spectral scan (200–325 nm) of M12.3. Spectral scan (200–800 nm) of M12.3 showed no evidence of absorbance at greater than 280 nm (data not shown). Spectral data indicate the presence of only a single molecular species in M12.3 preparation due to the absence of multiple spectra.

(C) LC-ToF absorbance profile of M12.3 (injection volume: 10 μl).

(D) Mass spectrum of M12.3 (compound **4**, inset) showing $(M+H)^+$ of 263.1027 and $(M+Na)^+$ of 285.0846.

(E) Mass spectrum of M12.3 and ^{13}C-labeled M12.3 showing $(M+H)^+$ of 263.1025 and 264.1057, respectively, in 1:1 ratio.

See also Figures S1 and S2–S9.

A. fumigatus gliZ mutant with the *gliZ* coding sequence. Moreover, complementation of a *gliP* mutant of *A. fumigatus* with *gliP* also restored gliotoxin biosynthesis and secretion (Cramer et al., 2006; Kupfahl et al., 2006).

Secreted metabolites may be involved in maintenance of competitive advantage against other fungi, and it has been speculated that toxin-resistance genes may exist in fungi to protect against the autotoxicity of such metabolites (Losada et al., 2009). Given the role of GSTs in reactive metabolite detoxification in animals, plants, and fungi (Hayes et al., 2005; Dixon et al., 2010; Burns et al., 2005), it was conceivable that *gliG* is involved in auto-protection against gliotoxin, as has previously been demonstrated by expression of *A. fumigatus gliA* in *L. maculans* (Gardiner et al., 2005a). However, *A. fumigatus* Δ*gliG*^{AF293} did not exhibit increased sensitivity to gliotoxin compared to *A. fumigatus* wild-type. Thus, *gliG*, and most likely all orthologs found in other ascomycetes (Patron et al., 2007; Fox and Howlett, 2008), does not appear to be primarily involved in self-protection against gliotoxin. This observation prompted us to investigate a role for *gliG* in gliotoxin biosynthesis.

Although Balibar and Walsh (2006) have shown that GliP can assemble 6-benzyl-3-hydroxymethylpiperazine-2,5-dione **2** (Figure 1) from L-Phe and L-Ser, it is unclear whether this diketopiperazine is an intermediate in gliotoxin biosynthesis. Indeed, to our knowledge, no free reaction intermediates in gliotoxin biosynthesis have been detected to date, as previously noted by Fox and Howlett (2008). Herein we report that 6-benzyl-6-hydroxy-1-methoxy-3-methylenepiperazine-2,5-dione **4** accumulates in and is secreted by a *gliG* mutant of *A. fumigatus*. Based on the structural similarity of **4** to **1** and **2**, it seems likely that **4** is a shunt metabolite from the gliotoxin biosynthetic pathway. We hypothesize that 6-benzyl-3-hydroxymethylpiperazine-2,5-dione **2** undergoes hydroxylation at C-6, catalyzed by the cytochrome P450s GliC or GliF to yield **5** (Figure 1). Hydroxylation of **5** at N-1, catalyzed either by GliC/GliF or more likely a nonspecific monooxygenase not encoded by a gene within the gliotoxin biosynthetic gene cluster, followed by O-methylation, perhaps catalyzed by GliM, and elimination of water from C-3/C-7 would give the shunt metabolite **4** (Figure 1). It is possible that N1 functionalization could be off

Table 1. NMR Data for M12.3 (6-benzyl-6-hydroxy-1-methoxy-3-methylenepiperazine-2,5-dione 4) in CD_3CN Unless Indicated

Position	^1H (mult, *J* in Hz)	^{13}C (mult)	HMBC (H to C)
1(N)-OCH_3	3.63 (s)	62.2 (q)	
2		157.2 (s)	
3		134.2 (s)	
4-NH	7.23[a]		
4-NH[b]	7.50[b]		C-5, 3[b]
5		161.1 (s)	
6		83.5 (s)	
6-OH	4.93 (s)		C-6, 8
7	5.00 (s), 5.33 (s)	100.1 (t)	C-2, 3
8	2.97–3.02 (d, 13.3)	46.5 (t)	C-5, 6, 9, 10, 14
	3.39–3.44 (d, 13.3)		
9		134.5 (s)	
10, 14	7.17–7.29 (m)[c]	131.4 (d)[d]	
11, 13	7.17–7.29 (m)[c]	129.1 (d)[d]	
12	7.17–7.29 (m)[c]	128.2 (d)	

[a] Overlapping the signals of the phenyl group.
[b] In $CDCl_3$.
[c] Overlapping the NH signal.
[d] Assignments of carbons are interchangeable.

pathway and be a self-protecting detoxification against the reactive intermediate. GliC/GliF-catalyzed hydroxylation of **5** at C-3 would afford **6**, which can lose two molecules of water to yield the 2,5-pyrazinedione **7** (Figure 1). GliG-catalyzed addition of two molecules of glutathione to **7** would yield **8** (Figure 1). An alternative sequence of reactions involving two rounds of sequential C-hydroxylation, water elimination, and glutathione addition reactions on **2** to give **8** is equally plausible. GliJ, a putative dipeptidase, is proposed to catalyze hydrolytic removal of the Glu residues in **8** to give **9** (Figure 1). GliI is similar to pyridoxal phosphate (PLP)-dependent enzymes such as 1-aminocyclopropane-1-carboxylate (ACC) synthase, which catalyzes a pyridoxal-mediated 1, 3-elimination reaction of S-adenosylmethionine to form ACC and 5′-deoxy-5′-methylthioadenosine (Fox and Howlett, 2008). The GliJ-mediated "deprotection" of the cysteine amino groups allows their condensation with GliI-bound PLP. Thus, we propose that GliI catalyzes two pyridoxal-mediated α, β-elimination reactions of **9** to afford 6-benzyl-3-hydroxymethylpiperazine-2,5-dione-3, 6-dithiol **10** (Figure 1). GliN-catalyzed N-4 methylation of **10**, followed by epoxidation of the phenyl group, catalyzed by the putative cytochrome P450s GliC or GliF, and epoxide opening with N-1, would yield reduced gliotoxin **3**, which has been reported to undergo GliT, FAD, and O_2-mediated oxidation to form gliotoxin **1** (Figure 1) (Wang et al., 2009; Schrettl et al., 2010; Scharf et al., 2010). It is conceivable that the GliJ- and GliI-catalyzed reactions to expose the thiol groups in **3** may occur after N-4 methylation and epoxidation/epoxide opening, given the potential deleterious effects of intracellular gliotoxin, due to the presence of reactive thiols or a disulfide bridge capable of redox cycling (Waring et al., 1995; Bernardo et al., 2003; Gardiner et al., 2005b; Nishida et al., 2005).

GSTs form homodimers (Sheehan et al., 2001). Nonreducing SDS-PAGE analysis of rGliG identified homodimeric and monomeric forms, indicating that rGliG is, like other GSTs, homodimeric. Activity of rGliG toward EPNP, CDNB, and DCNB was observed, verifying the predicted GST activity of this enzyme. GliG exhibited higher activity toward both CDNB and DCNB than GstA, GstB, and GstC, previously cloned and expressed from *A. fumigatus* (Burns et al., 2005). In fact, GstA, GstB, and GstC did not have detectable activity toward DCNB. Interestingly, a low but detectable glutathione reductase activity was observed for rGliG. Although rGliG did not exhibit glutathione peroxidase activity, this was detectable for positive control enzyme, *A. fumigatus* GstB (Burns et al., 2005). Thus, it appears that rGliG exhibits a different pattern of reactivity to other *A. fumigatus* GSTs.

In conclusion we show that the GST, GliG, is involved in the biosynthesis of gliotoxin and not in self-resistance to this ETP. GliG-mediated addition of glutathione to acyl imine-containing intermediates is proposed to be a key step in gliotoxin biosynthesis. To our knowledge, this is the first time that such a reaction has been suggested to play a pivotal function in ETP biosynthesis.

SIGNIFICANCE

Most studies pertaining to gliotoxin have focused on its role in mediating fungal virulence and the mechanisms of action by which this occurs. Although the roles of GliP and GliT in the first and last steps of gliotoxin biosynthesis, respectively, have been investigated in vitro and in vivo, to our knowledge, no further information on gliotoxin biosynthesis has been forthcoming. Here, we demonstrate that disruption of *gliG* within the gliotoxin biosynthetic gene cluster of *A. fumigatus* results in the secretion of a shunt metabolite from the gliotoxin biosynthetic pathway, 6-benzyl-6-hydroxy-1-methoxy-3-methylenepiperazine-2,5-dione. We show that GliG exhibits glutathione S-transferase activity, and the presence of a hydroxyl group at C-6 of the shunt metabolite leads us to propose that elimination of water from N-1/C-6 of a C-6 hydroxylated piperazine-2,5-dione intermediate yields an acyl imine, which undergoes GliG-mediated addition of glutathione. A similar hydroxylation, elimination, glutathione addition sequence is proposed to occur at C-3 of the piperazine-2,5-dione. We propose that the subsequent peptidase activity of GliJ, and PLP-dependent thiol elimination catalyzed by GliI, results in formation of a dithiol intermediate. In the absence of GliG, the shunt metabolite is likely formed due to the metabolic instability of the presumed 6-benzyl-6-hydroxy-3-hydroxymethylpiperazine-2,5-dione biosynthetic intermediate. We propose that N-4 methylation and epoxidation of the phenyl group occur after thiolation because both modifications are absent in 6-benzyl-6-hydroxy-1-methoxy-3-methylenepiperazine-2,5-dione. GliG does not play a role in self-protection of *A. fumigatus* against exogenous gliotoxin, unlike GliT, a gliotoxin reductase/oxidase, which has been demonstrated to be the key enzyme responsible for this phenomenon. Overall, these results elucidate a catalytic role for GliG in gliotoxin biosynthesis.

EXPERIMENTAL PROCEDURES

Strains, Growth Conditions, and General DNA Manipulation

In general, *A. fumigatus* strains (Table S1) were grown at 37°C in *Aspergillus* minimal media (AMM). AMM contained 1% (w/v) glucose as carbon-source, 20 mM L-glutamine as nitrogen-source, and trace elements according to Pontecorvo et al. (1953).

Gene Deletion and Complementation in *A. fumigatus*

For generating Δ*gliG* strains, the bipartite marker technique was used (Nielsen et al., 2006). Primer details are provided in Table S2. Briefly, *A. fumigatus* strains AF293 and *akuB* were cotransformed with two DNA constructs, each containing an incomplete fragment of a pyrithiamine resistance gene (*ptrA*) (Tilburn et al., 2005; Kubodera et al., 2000) fused to 1.0 and 1.2 kb of *gliG*-flanking sequences, respectively. Further details and the *gliG* complementation strategy are given in Supplemental Experimental Procedures.

Northern Analysis

RNA was isolated using TRI-Reagent (Sigma-Aldrich). Equal concentrations of total RNA (10 μg) were size separated on 1.2% (w/v) agarose-2.2 M formaldehyde gels and blotted onto Hybond N+ membranes (Amersham Biosciences). The hybridization probes used in this study were generated by PCR using primers ogliG-7 and ogliG-8.

Phenotypic Analysis of *A. fumigatus* AF293 Wild-Type and Δ*gliG* Strains

Relative sensitivities of *A. fumigatus* wild-type, Δ*gliG*, and *gliG*^{c} were assessed against gliotoxin (10–50 μg/ml) (Schrettl et al., 2010; Losada et al., 2009), voriconazole (0.15 and 0.25 μg/ml), H_2O_2 (1, 2, and 5 mM), and amphotericin B (1, 2, and 5 μg/ml). See Supplemental Experimental Procedures for further details.

Virulence Model

G. mellonella larvae (n = 10) were inoculated into the hind pro-leg with 10^6 *A. fumigatus* conidia in 20 μl (per larva) (Reeves et al., 2004). Mortality rates were recorded for 72 hr postinjection. See Supplemental Experimental Procedures for further details.

Analysis of Gliotoxin Production

To analyze gliotoxin production, *A. fumigatus* wild-type, Δ*gliG* and complemented strains were grown at 37°C for 72 hr in AMM. Supernatants were chloroform extracted, and fractions were evaporated to complete dryness, followed by resolubilization in methanol and analysis by RP-HPLC or LC-MS, as described by Reeves et al. (2004) and Schrettl et al. (2010).

LC-MS Analysis

Electrospray MS analysis of gliotoxin was performed as described previously (Schrettl et al., 2010). LC-ToF MS was performed on an Agilent HPLC 1200 series and injected (injection volume: 10 μl) using electrospray ionization inputted into a time-of-flight chamber (Agilent). The LC separation was done on a XDB C_{18} column (4.6 × 150 mm) using a water/acetonitrile (both containing 0.1% [v/v] formic acid) gradient at a flow rate of 0.5 ml/min. The gradient was started at 50% (v/v) acetonitrile, which was increased to 100% acetonitrile in 10 min; 100% acetonitrile was maintained for 5 min before the gradient was returned to starting conditions. Spectra were collected at 0.99 spectra per second.

Extraction and Purification of the Gliotoxin Shunt Metabolite

A. fumigatus Δ*gliG* cultures were grown at 37°C for 48 hr in AMM. Culture supernatants were extracted twice with chloroform. Organic extracts were evaporated to dryness and resolubilized in methanol. A layer of the methanolic solution was applied to preparative TLC plates (Silica gel, UV 254 nm, 20 × 20 cm, 50 μm; Analtech, Newark, DE, USA). Plates were developed with two runs of dichloromethane:methanol (97:3 containing 0.5% [v/v] acetic acid). The silica in the area containing metabolite M12.3 was collected and washed in acetone (20 ml), dried, and the resultant material was resolubilized in either CD_3CN or $CDCl_3$ for NMR analysis.

Incorporation of [3-^{13}C]L-Phe into M12.3 (Compound 4)

[3-^{13}C]L-Phe (10 mg) was added to 24-hr cultures of *A. fumigatus* Δ*gliG* (10 ml). The culture supernatants were harvested after a further 24 hr of incubation, and M12.3 was purified as described above.

NMR Spectroscopic Analysis

^{1}H, ^{13}C, DEPT, COSY, HSQC, and HMBC-NMR spectra were recorded in CD_3CN or $CDCl_3$, on a Bruker Avance AV300 spectrometer operating at 300 MHz for the ^{1}H nucleus and 75 MHz for the ^{13}C nucleus. ^{1}H and ^{13}C-NMR spectra were also obtained at 500 and 125 MHz, respectively, on a Bruker Avance III 500 MHz spectrometer at 25°C. Chemical shifts are reported in ppm referenced to residual protonated solvent.

Reductive Alkylation of Gliotoxin

An alkylation strategy to specifically label free thiols was used to determine the presence of sulfydryl residues, either prior to or post-reduction with $NaBH_4$, in gliotoxin or related metabolites. Briefly, organic extracts of culture supernatants from *A. fumigatus* AF293, Δ*gliG*^{AF293}, and *gliG*^{C} (100 μl), respectively, were treated for 1 hr with $NaBH_4$ (50 mM final) to reduce disulfide bridges prior to alkylation using 5′-iodoacetamidofluorescein (400 nmol) to yield diacetamidofluorescein-gliotoxin (GT-$(AF)_2$), which was identified by RP-HPLC analysis (Schrettl et al., 2010).

GliG Expression and Activity Analysis

The *gliG* coding sequence was amplified from *A. fumigatus* cDNA using primers gliG-F and gliG-R, respectively (Table S2), and cloned into a pProEx-Htb vector (Invitrogen). Expression in, and purification from, *E. coli* was undertaken as previously described for *A. fumigatus* GstA-C (Burns et al., 2005). GST, and related enzyme activities were determined as previously described (Burns et al., 2005; Habdous et al., 2002; Hoque et al., 2007).Methodology used for protein isolation from *A. fumigatus* (Carberry et al., 2006; Bradford, 1976) is given in the Supplemental Experimental Procedures.

SUPPLEMENTAL INFORMATION

Supplemental Information includes Supplemental Experimental Procedures, ten figures, and two tables and can be found with this article online at doi:10.1016/j.chembiol.2010.12.022.

ACKNOWLEDGMENTS

This work was funded by a Science Foundation Ireland Research Frontiers Project Grant (RFP/GEN/F571). S.C. was funded by PRTLI, Cycle 4. M.S. was a recipient of a Marie Curie Fellowship. S.M.B. was supported by a grant from the UK BBSRC to G.L.C. (Grant ref. BB/H006281/1). LC facilities were funded by the Higher Education Authority, and MALDI-ToF instrument was funded by the Health Research Board. We are grateful to Dr. Ann Connolly, University College Dublin, who carried out elemental analyses, Orla Fenelon and Barbara Woods, NUI Maynooth, who carried out LC-ToF MS analyses, and Dr. Padraig McLoughlin, Teagasc Ashtown Food Research Centre, Dublin, who performed some of the NMR analyses. None of the authors of this manuscript has a financial interest related to this work.

Received: May 31, 2010
Revised: December 15, 2010
Accepted: December 29, 2010
Published: April 21, 2011

REFERENCES

Balibar, C.J., and Walsh, C.T. (2006). GliP, a multimodular nonribosomal peptide synthetase in *Aspergillus fumigatus*, makes the diketopiperazine scaffold of gliotoxin. Biochemistry *45*, 15029–15038.

Bernardo, P.H., Brasch, N., Chai, C.L., and Waring, P. (2003). A novel redox mechanism for the glutathione-dependent reversible uptake of a fungal toxin in cells. J. Biol. Chem. *278*, 46549–46555.

Bok, J.W., Chung, D., Balajee, S.A., Marr, K.A., Andes, D., Nielsen, K.F., Frisvad, J.C., Kirby, K.A., and Keller, N.P. (2006). GliZ, a transcriptional regulator of gliotoxin biosynthesis, contributes to *Aspergillus fumigatus* virulence. Infect. Immun. *74*, 6761–6768.

Bradford, M.M. (1976). A rapid and sensitive method for the quantitation of microgram quantities of protein utilizing the principle of protein-dye binding. Anal. Biochem. *72*, 248–254.

Burns, C., Geraghty, R., Neville, C., Murphy, A., Kavanagh, K., and Doyle, S. (2005). Identification, cloning, and functional expression of three glutathione transferase genes from *Aspergillus fumigatus*. Fungal Genet. Biol. *42*, 319–327.

Buysens, K.J., Vandenberghe, D.D., Toppet, S.M., and Hoornaert, G.J. (1996). Generation of 6-alkylidene/benzylidene-3,6-dihydropyrazin-2(1*H*)ones by reaction of 6-bromomethylpyrazin-2(1*H*)-ones with methoxide and further conversion into specific piperazine-2,5-diones and pyrazin-2(1*H*)-ones. J. Chem. Soc. Perkin Trans. I, 231–237.

Carberry, S., Neville, C.M., Kavanagh, K.A., and Doyle, S. (2006). Analysis of major intracellular proteins of *Aspergillus fumigatus* by MALDI mass spectrometry: identification and characterisation of an elongation factor 1B protein with glutathione transferase activity. Biochem. Biophys. Res. Commun. *341*, 1096–1104.

Choi, H.S., Shim, J.S., Kim, J.A., Kang, S.W., and Kwon, H.J. (2007). Discovery of gliotoxin as a new small molecule targeting thioredoxin redox system. Biochem. Biophys. Res. Commun. *359*, 523–528.

Cramer, R.A., Jr., Gamcsik, M.P., Brooking, R.M., Najvar, L.K., Kirkpatrick, W.R., Patterson, T.F., Balibar, C.J., Graybill, J.R., Perfect, J.R., Abraham, S.N., et al. (2006). Disruption of a nonribosomal peptide synthetase in *Aspergillus fumigatus* eliminates gliotoxin production. Eukaryot. Cell *5*, 972–980.

da Silva Ferreira, M.E., Kress, M.R., Savoldi, M., Goldman, M.H., Härtl, A., Heinekamp, T., Brakhage, A.A., and Goldman, G.H. (2006). The *akuB*(KU80) mutant deficient for nonhomologous end joining is a powerful tool for analyzing pathogenicity in *Aspergillus fumigatus*. Eukaryot. Cell *5*, 207–211.

Dixon, D.P., Skipsey, M., and Edwards, R. (2010). Roles for glutathione transferases in plant secondary metabolism. Phytochemistry *71*, 338–350.

Fox, E.M., and Howlett, B.J. (2008). Biosynthetic gene clusters for epipolythiodioxopiperazines in filamentous fungi. Mycol. Res. *112*, 162–169.

Gardiner, D.M., and Howlett, B.J. (2005). Bioinformatic and expression analysis of the putative gliotoxin biosynthetic gene cluster of *Aspergillus fumigatus*. FEMS Microbiol. Lett. *248*, 241–248.

Gardiner, D.M., Cozijnsen, A.J., Wilson, L.M., Pedras, M.S., and Howlett, B.J. (2004). The sirodesmin biosynthetic gene cluster of the plant pathogenic fungus *Leptosphaeria maculans*. Mol. Microbiol. *53*, 1307–1318.

Gardiner, D.M., Jarvis, R.S., and Howlett, B.J. (2005a). The ABC transporter gene in the sirodesmin biosynthetic gene cluster of *Leptosphaeria maculans* is not essential for sirodesmin production but facilitates self-protection. Fungal Genet. Biol. *42*, 257–263.

Gardiner, D.M., Waring, P., and Howlett, B.J. (2005b). The epipolythiodioxopiperazine (ETP) class of fungal toxins: distribution, mode of action, functions and biosynthesis. Microbiology *151*, 1021–1032.

Habdous, M., Vincent-Viry, M., Visvikis, S., and Siest, G. (2002). Rapid spectrophotometric method for serum glutathione S-transferases activity. Clin. Chim. Acta *326*, 131–142.

Hayes, J.D., Flanagan, J.U., and Jowsey, I.R. (2005). Glutathione transferases. Annu. Rev. Pharmacol. Toxicol. *45*, 51–88.

Hoque, E., Pflugmacher, S., Fritscher, J., and Wolf, M. (2007). Induction of glutathione S-transferase in biofilms and germinating spores of *Mucor hiemalis* strain EH5 from cold sulfidic spring waters. Appl. Environ. Microbiol. *73*, 2697–2707.

Kim, J., Ashenhurst, J.A., and Movassaghi, M. (2009). Total synthesis of (+)-11,11′-dideoxyverticillin A. Science *324*, 238–241.

King, R.R., Lawrence, C.H., Embleton, J., and Calhoun, L.A. (2003). More chemistry of the thaxtomin phytotoxins. Phytochemistry *64*, 1091–1096.

Kubodera, T., Yamashita, N., and Nishimura, A. (2000). Pyrithiamine resistance gene (*ptrA*) of *Aspergillus oryzae*: cloning, characterization and application as a dominant selectable marker for transformation. Biosci. Biotechnol. Biochem. *64*, 1416–1421.

Kupfahl, C., Heinekamp, T., Geginat, G., Ruppert, T., Hartl, A., Hof, H., and Brakhage, A.A. (2006). Deletion of the gliP gene of *Aspergillus fumigatus* results in loss of gliotoxin production but has no effect on virulence of the fungus in a low-dose mouse infection model. Mol. Microbiol. *62*, 292–302.

Lewis, R.E., Wiederhold, N.P., Chi, J., Han, X.Y., Komanduri, K.V., Kontoyiannis, D.P., and Prince, R.A. (2005). Detection of gliotoxin in experimental and human aspergillosis. Infect. Immun. *73*, 635–637.

Li, X., Kim, S.K., Nam, K.W., Kang, J.S., Choi, H.D., and Son, B.W. (2006). A new antibacterial dioxopiperazine alkaloid related to gliotoxin from a marine isolate of the fungus *Pseudallescheria*. J. Antibiot. (Tokyo) *59*, 248–250.

Losada, L., Ajayi, O., Frisvad, J.C., Yu, J., and Nierman, W.C. (2009). Effect of competition on the production and activity of secondary metabolites in *Aspergillus* species. Med. Mycol. *47* (*Suppl 1*), S88–S96.

Maiya, S., Grundmann, A., Li, S.M., and Turner, G. (2006). The fumitremorgin gene cluster of *Aspergillus fumigatus*: identification of a gene encoding brevianamide F synthetase. ChemBioChem *7*, 1062–1069.

Morel, M., Ngadin, A.A., Droux, M., Jacquot, J.P., and Gelhaye, E. (2009). The fungal glutathione *S*-transferase system. Evidence of new classes in the wood-degrading basidiomycete *Phanerochaete chrysosporium*. Cell. Mol. Life Sci. *66*, 3711–3725.

Nielsen, M.L., Albertsen, L., Lettier, G., Nielsen, J.B., and Mortensen, U.H. (2006). Efficient PCR-based gene targeting with a recyclable marker for *Aspergillus nidulans*. Fungal Genet. Biol. *43*, 54–64.

Nierman, W.C., Pain, A., Anderson, M.J., Wortman, J.R., Kim, H.S., Arroyo, J., Berriman, M., Abe, K., Archer, D.B., Bermejo, C., et al. (2005). Genomic sequence of the pathogenic and allergenic filamentous fungus *Aspergillus fumigatus*. Nature *438*, 1151–1156.

Nishida, S., Yoshida, L.S., Shimoyama, T., Nunoi, H., Kobayashi, T., and Tsunawaki, S. (2005). Fungal metabolite gliotoxin targets flavocytochrome b558 in the activation of the human neutrophil NADPH oxidase. Infect. Immun. *73*, 235–244.

Patron, N.J., Waller, R.F., Cozijnsen, A.J., Straney, D.C., Gardiner, D.M., Nierman, W.C., and Howlett, B.J. (2007). Origin and distribution of epipolythiodioxopiperazine (ETP) gene clusters in filamentous ascomycetes. BMC Evol. Biol. *7*, 174.

Pedras, M.S., and Yang, Y. (2009). Mapping the sirodesmin PL biosynthetic pathway—a remarkable intrinsic steric deuterium isotope effect on a 1H NMR chemical shift determines β-proton exchange in tyrosine. Can. J. Chem. *87*, 556–562.

Pena, G.A., Pereyra, C.M., Armando, M.R., Chiacchiera, S.M., Magnoli, C.E., Orlando, J.L., Dalcero, A.M., Rosa, C.A., and Cavaglieri, L.R. (2010). *Aspergillus fumigatus* toxicity and gliotoxin levels in feedstuff for domestic animals and pets in Argentina. Lett. Appl. Microbiol. *50*, 77–81.

Pontecorvo, G., Roper, J.A., Hemmons, L.M., Macdonald, K.D., and Bufton, A.W. (1953). The genetics of *Aspergillus nidulans*. Adv. Genet. *5*, 141–238.

Reeves, E.P., Messina, C.G., Doyle, S., and Kavanagh, K. (2004). Correlation between gliotoxin production and virulence of *Aspergillus fumigatus* in *Galleria mellonella*. Mycopathologia *158*, 73–79.

Scharf, D.H., Remme, N., Heinekamp, T., Hortschansky, P., Brakhage, A.A., and Hertweck, C. (2010). Transannular disulfide formation in gliotoxin biosynthesis and its role in self-resistance of the human pathogen *Aspergillus fumigatus*. J. Am. Chem. Soc. *132*, 10136–10141.

Schrettl, M., Carberry, S., Kavanagh, K., Haas, H., Jones, G.W., O'Brien, J., Stephens, J., Fenelon, O., Nolan, A., and Doyle, S. (2010). Self-protection against gliotoxin—a component of the gliotoxin biosynthetic cluster, GliT, completely protects *Aspergillus fumigatus* against exogenous gliotoxin. PLoS Pathog. *6*, e1000952.

Sheehan, D., Meade, G., Foley, V.M., and Dowd, C.A. (2001). Structure, function and evolution of glutathione transferases: implications for classification of non-mammalian members of an ancient enzyme superfamily. Biochem. J. *360*, 1–16.

Shin, C.-G., Nanjo, K., Kato, M., and Yoshimura, J. (1975). α,β-Unsaturated carboxylic acid derivatives. IX. The cyclization of α-(N-acyl-hydroxyamino) acid esters with ammonia or hydroxylamine. Bull. Chem. Soc. Jpn. *48*, 2584–2587.

Stack, D., Neville, C.M., and Doyle, S. (2007). Nonribosomal peptide synthesis in the human pathogen *Aspergillus fumigatus* and other fungi. Microbiology *153*, 1297–1306.

Tilburn, J., Sanchez-Ferrero, J.C., Reoyo, E., Arst, H.N., Jr., and Penalva, M.A. (2005). Mutational analysis of the pH signal transduction component PalC of *Aspergillus nidulans* supports distant similarity to BRO1 domain family members. Genetics *171*, 393–401.

Wang, C., Wesener, S.R., Zhang, H., and Cheng, Y.Q. (2009). An FAD-dependent pyridine nucleotide-disulfide oxidoreductase is involved in disulfide bond formation in FK228 anticancer depsipeptide. Chem. Biol. *16*, 585–593.

Waring, P., Sjaarda, A., and Lin, Q.H. (1995). Gliotoxin inactivates alcohol dehydrogenase by either covalent modification or free radical damage mediated by redox cycling. Biochem. Pharmacol. *49*, 1195–1201.

Woodcock, J.C., Henderson, W., and Miles, C.O. (2001). Metal complexes of the mycotoxins sporidesmin A and gliotoxin, investigated by electrospray ionisation mass spectrometry. J. Inorg. Biochem. *85*, 187–199.

